Device results: Typical device *I/V* characteristics are shown in Fig. 3, indicating a sharp forward turn-on characteristic with low reverse leakage and a breakdown voltage in the range

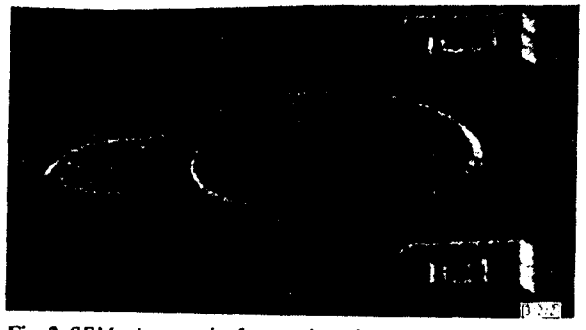

Fig. 2 *SEM micrograph of a complete photodiode*

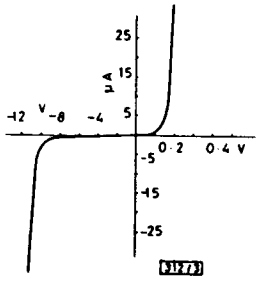

Fig. 3 *Current/voltage characteristics for a device of* $1{\cdot}8 \times 10^{-4}\,cm^2$ *junction area*

10–12 V. Dark currents (at ambient temperatures) as low as 35 nA have been obtained at −0·5 V bias. This value is three orders of magnitude lower than devices of similar area and composition fabricated by Poulain *et al.*,[1] who did not incorporate a graded layer to accommodate the lattice mismatch. In addition, this value of leakage is substantially lower than the value of 10 μA obtained by Bowers *et al.*[3] for similar geometry devices with lattice-matched GaInAsSb/GaSb photodetectors operating over the same wavelength range. The detailed *I/V* characteristics indicate that the breakdown occurring at 10–12 V is due to a tunnelling component, consistent with predicted performance for this alloy composition and doping level. Typical capacitance values of 4 pF are obtained with this structure at −0·5 V bias, with a forward resistance of less than 3 Ω.

The spectral dependence of the responsivity is shown in Fig. 4, indicating a broadband response with peak efficiency

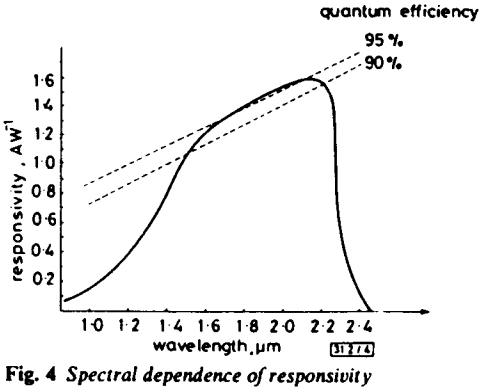

Fig. 4 *Spectral dependence of responsivity*

as high as 95% over the 1·7–2·25 μm wavelength range, with a long-wavelength cutoff at 2·4 μm. This compares with peak values of 20% efficiency obtained by Poulain *et al.*[1] at 2–2·2 μm and 55% obtained by Bowers *et al.*[3] for wavelengths up to 2·2 μm. At shorter wavelengths a rapid decrease in efficiency with decreasing wavelength occurs owing to carrier recombination in the p^+ layer for wavelengths shorter than the band-edge of the AlInAs layer. Uniformity of response over the device active area has been measured with a scanning laser system and shown to be better than 3% over the active area.

Conclusions: High-quantum-efficiency, low-leakage-current GaInAs/AlInAs heterojunction photodiodes have been reported for detection at wavelengths extending to 2·4 μm. These results are, to the best of our knowledge, the highest values of quantum efficiency and lowest dark currents reported for photodiodes operating in this wavelength range, and demonstrate the potential of the graded buffer layer technique to tailor the bandgap of the GaInAs alloy to detector requirements over a wide range at long wavelengths. Extension of this approach is easily envisaged by increasing the In content of the active layer to give peak efficiency out to at least 3 μm.

Acknowledgments: This work has been carried out with the support of the Procurement Executive, UK Ministry of Defence, sponsored by DCVD.

A. J. MOSELEY
M. D. SCOTT
A. H. MOORE
R. H. WALLIS

Plessey Research (Caswell) Ltd.
Caswell
Towcester, Northants, NN12 8EQ, United Kingdom

8th September 1986

References

1 POULAIN, P., DE FORTE-POISSON, M. A., KAMIERSKI, K., and DE CREMOUX, B.: '$In_xGa_{1-x}As$ photodiodes for the 1·0 to 2·4 μm spectral region prepared by low-pressure MOCVD'. Inst. Phys. Conf. Ser. 74, 1985, p. 421; GaAs and related compounds, Biarritz, 1984

2 SUSSMANN, R. S., ASH, R. M., MOSELEY, A. J., and GOODFELLOW, R. C.: 'Ultra-low-capacitance flip-chip-bonded GaInAs PIN photodetector for long-wavelength high-data-rate fibre-optic systems', *Electron. Lett.*, 1985, **21**, pp. 593–595

3 BOWERS, J. E., SRIVASTAVA, A. K., BURRUS, C. A., DEWINTER, J. C., POLLACK, M. A., and ZYSKIND, J. L.: 'High-speed GaInAsSb/GaSb PIN photodetectors for wavelengths to 2·3 μm', *ibid.*, 1986, **22**, pp. 137–138

DEPENDENCE OF FUSED TAPER COUPLERS ON EXTERNAL REFRACTIVE INDEX

Indexing terms: Optical fibres, Optical couplers

We present the results of an experimental and theoretical investigation into the dependence of fused taper couplers on changes in the external refractive index. We show that it should be possible to fabricate long couplers which are insensitive to changes in the external refractive index.

Introduction: Single-mode fibre fused taper couplers are often embedded in a silicone resin to protect them from moisture and dust.[1,4] Unfortunately, the refractive index of the resin is temperature-dependent and this can cause the coupler to be very sensitive to temperature changes.[1,2] This is most noticeable in couplers pulled through many power exchanges for use in optical filters or wavelength-division multiplexers. It is often assumed that these effects are minimised by strong fusion, so that the coupler cross-section is oval in shape. In this letter we show that this is not the optimum shape and that weaker fusion results in a cross-sectional shape which will minimise temperature dependence.

To understand why this is so, consider a typical coupler cross-section (Fig. 1). To parameterise this shape we make AB, DE arcs of circles and BCD a semicircle. The degree of fusion is described by t. Neglecting the fibre cores, the coupling coefficient can be expressed as[3,5]

$$C = \left(\frac{\alpha_1 \lambda}{n_2 a^2} + \frac{\alpha_2 \lambda^2}{n_2 a^3 (n_2^2 - n_3^2)^{1/2}}\right) L_{eff} \qquad (1)$$

The taper length is L_{eff} and α_1, α_2 are dimensionless numbers depending only on a and t. As the degree of fusion changes from strong to weak α_2 will change from negative to positive,

and therefore at some point must vanish. The resulting coupler will be insensitive to external index changes.

Experimental results: We have checked the validity of eqn. 1 with measurements on strongly and weakly fused couplers. In Fig. 2 we show the variation of C with $(n_2^2 - n_3^2)^{-1/2}$ for several strongly fused couplers. C has been expressed in the

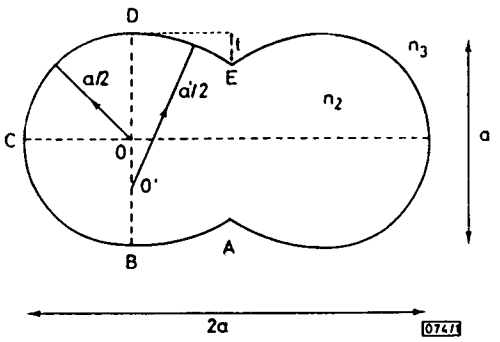

Fig. 1 *Diagrammatic representation of cross-section of a fused taper coupler*

The shape is parameterised by making AB and DE arcs of circles, centre O' and radius $a'/2$, and BCD a semicircle with centre O and radius $a/2$. The degree of fusion is described by t

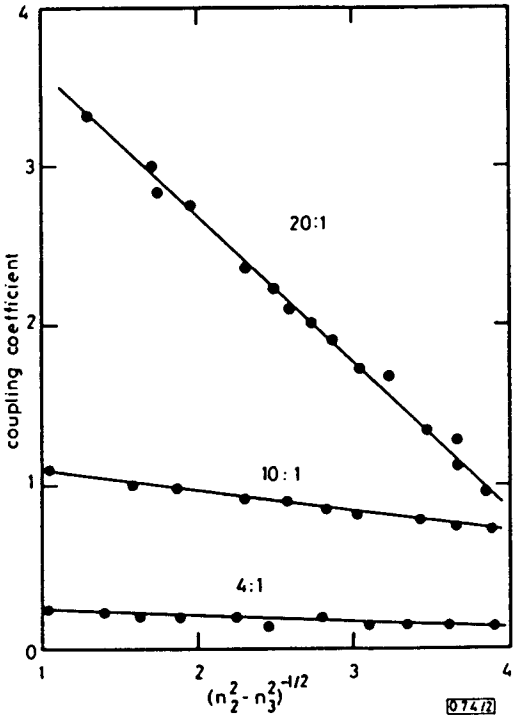

Fig. 2 *Experimental measurement of variation of coupling coefficient with external index n_3 for three strongly fused couplers with taper ratios of 20, 10 and 4*

range 0 to 2π. The straight-line dependence predicted by eqn. 1 is clearly obeyed. In Fig. 3 we have plotted the spectral period $\Delta\lambda$ against $(n_2^2 - n_3^2)^{-1/2}$ for a 70 mm weakly fused coupler. Eqn. 1 predicts a straight-line behaviour which is again shown by our measurements. These results clearly demonstrate the validity of the cladding mode model used to derive eqn. 1.

Analysis: A numerical effective index method[6] was used to calculate the coupling coefficient for the geometry of Fig. 1. In Fig. 4 we have plotted C/L_{eff} as a function of t for $a = 5\,\mu$m. Two curves are shown corresponding to $n_3 = 1$ and 1·42. At $t = 0{\cdot}955\,\mu$m the two curves intersect, corresponding to $\alpha_2 = 0$ referred to above. To verify this we have plotted in Fig. 5 C/L_{eff} against $(n_2^2 - n_3^2)^{-1/2}$ for $t = 0$ and $0{\cdot}955\,\mu$m. For $t = 0{\cdot}955\,\mu$m the coupling coefficient is almost independent of n_3 over the range $n_3 = 1$ to 1·44. Similar results are found for couplers with different cross-sectional areas.

Discussion: It is clear from Fig. 5 that a strongly fused coupler may show considerable variation as the external index is varied. This will cause many power exchanges in the output of

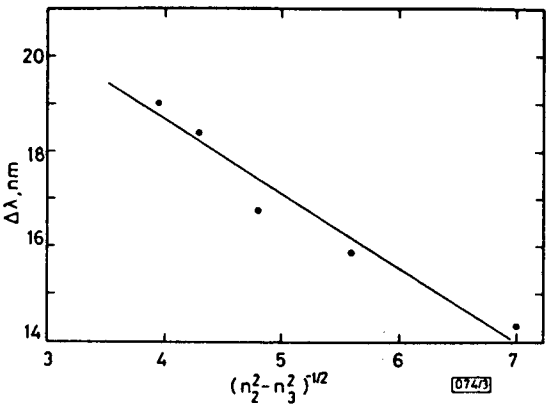

Fig. 3 *Average spectral period $\Delta\lambda$ as a function of $(n_2^2 - n_3^2)^{-1/2}$ for a weakly fused coupler with a 70 mm fused length*

Theory predicts a straight-line dependence

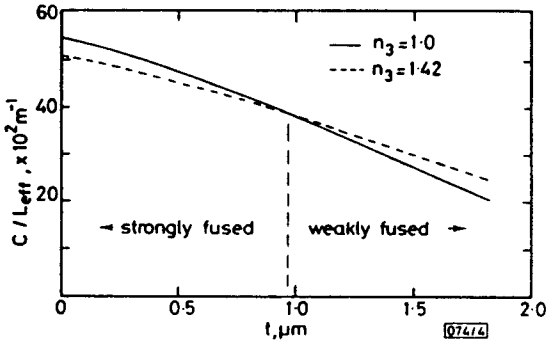

Fig. 4 *Theoretical variation of coupling coefficient as a function of t for cross-sectional shape shown in Fig. 1*

The curves plotted correspond to $a = 5\,\mu$m, $n_2 = 1{\cdot}458$ and $n_3 = 1{\cdot}0$ and 1·42. The wavelength assumed was 633 nm

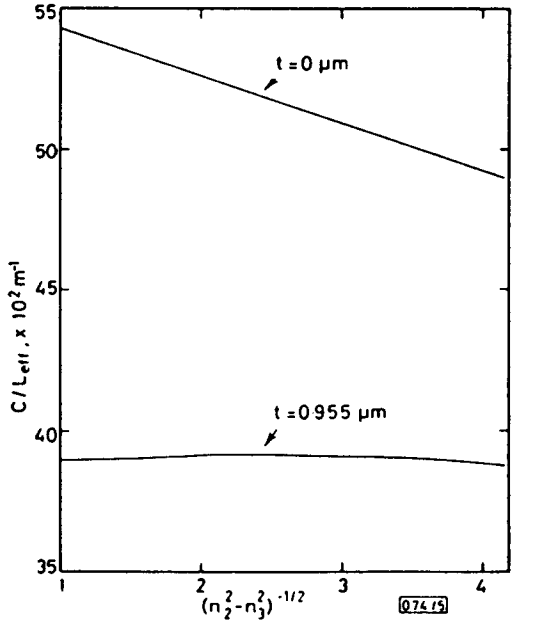

Fig. 5 *Theoretical variation of coupling coefficient as a function of $(n_2^2 - n_3^2)^{-1/2}$ for cross-sectional shape of Fig. 1*

The following parameters were assumed: $a = 5\,\mu$m, $n_2 = 1{\cdot}458$, wavelength = 633 nm. The two curves correspond to $t = 0$ and $0{\cdot}955\,\mu$m

a long coupler. For an optimally fused coupler there is almost no change in C over the same index range. Recently reported experiments suggest that such optimally fused couplers have already been fabricated accidentally.[2]

Conclusions: We have shown that the effects of external index variations on fused taper couplers are well described by a cladding mode picture. The degree of fusion has a strong effect on the coupler behaviour and there is an optimal shape of the coupler cross-section that will result in couplers which are insensitive to changes in external index.

F. P. PAYNE

Department of Engineering
Cambridge University
Trumpington Street, Cambridge CB2 1PZ, United Kingdom

T. FINEGAN

Department of Electrical Engineering & Electronics
Liverpool University
Brownlow Hill, Liverpool L69 3BX, United Kingdom

M. S. YATAKI
R. J. MEARS
C. D. HUSSEY

Department of Electronics & Information Engineering
University of Southampton
Highfield, Southampton SO9 5NH, United Kingdom

16th July 1986

References

1 DE FORNEL, F., RAGDALE, C. M., and MEARS, R. J.: 'Analysis of single-mode fused tapered couplers', *IEE Proc. J., Optoelectron.*, 1985, **131**, pp. 221–228
2 LAMONT, R. G., JOHNSON, D. C., and HILL, K. O.: 'Power transfer in fused biconical-taper single-mode fibre couplers: dependence on external refractive index', *Appl. Opt.*, 1985, **24**, pp. 327–332
3 PAYNE, F. P., HUSSEY, C. D., and YATAKI, M. S.: 'Modelling fused single-mode-fibre couplers', *Electron. Lett.*, 1985, **21**, pp. 461–462
4 BRICHENO, T., and FIELDING, A.: 'Stable low-loss single-mode couplers', *ibid.*, 1984, **20**, pp. 230–232
5 SNYDER, A. W., and XHENG, X.: 'Optical fibers of arbitrary cross sections', *J. Opt. Soc. Am.*, 1986, **3**, to be published
6 ADAMS, M. J.: 'An introduction to optical waveguides' (John Wiley, 1981), pp. 188–212

ERRATA

Authors' corrections

FARIDIAN, F., SOMEKH, M. G., and SAKAI, I.: 'New CW imaging mode for scanning acoustic microscopy', *Electron. Lett.*, 1986, **22**, (15), pp. 800–802

In lines 8, 9 and 13 of the second column of p. 801, the variables should read:

$$A_n(\omega), \left[\sum_n A_n^2(\omega)\right]^{1/2} \text{ and } \left[\sum_n \omega^2 A_n^2(\omega)\right]^{1/2}$$

respectively

VIBET, C.: 'Properties of master/slave manipulators', *Electron. Lett.*, 1986, **22**, (19), pp. 1019–1020

The second line of eqn. 1 and eqn. 14 should read:

$$A_S\ddot{\theta}_S + D_S(\theta_S, \dot{\theta}_S) + Q_S(\theta_S) = T_S + T_e$$

and

$$E = (K_M + K_S)^{-1}[J_M^T F_0 - J_S^T(F_e + M_e g)]$$

respectively. The line following eqn. 13 should read:

where F_e^0 and $M_e^0 g \ldots$

Editorial corrections

HIGASHIMURA, M., and FUKUI, Y.: 'Novel lossless tunable floating FDNR simulation using two current conveyors and a buffer', *Electron. Lett.*, 1986, **22**, (18), pp. 938–939

On p. 939, in Fig. 1*b*, '-1' should read: '$+1$'

In the last line of the second author's address, 'Torrori' should read: 'Tottori'